

**Synthesis, characterization, crystal structures and computational studies on novel cyrhetyrenyl hydrazones**

Johana Gómez <sup>a</sup>, Nelson Leiva <sup>a</sup>, Rodrigo Arancibia <sup>a</sup>, Juan Oyarzo <sup>a</sup>, Gonzalo E. Buono-Core <sup>a</sup>, A. Hugo Klahn <sup>a, \*, 1</sup>, Vania Artigas <sup>a</sup>, Mauricio Fuentealba <sup>a</sup>, Ramon Bosque <sup>b</sup>, Gabriel Aullón <sup>b</sup>, Concepción López <sup>b, \*\*, 1</sup>, Mercè Font-Bardía <sup>c</sup>, Teresa Calvet <sup>d</sup>

a Instituto de Química, Pontificia Universidad Católica de Valparaíso, Casilla 4059, Valparaíso, Chile  
b Departament de Química Inorgànica, Facultat de Química, Universitat de Barcelona, Martí i Franquès 1-11, E-08028 Barcelona, Spain  
c Unitat de Difracció de Raigs-X, Centres Científics i Tecnològics (CCiT), Universitat de Barcelona, Solè i Sabaris 1-3, E-08028 Barcelona, Spain  
d Departament de Cristal·lografia, Mineralogia i Dipòsits Minerals, Facultat de Geologia, Universitat de Barcelona, Martí i Franquès s/n, E-08028 Barcelona, Spain

\* Corresponding author.

\*\* Corresponding author.

E-mail addresses: [hugo.klahn@pucv.cl](mailto:hugo.klahn@pucv.cl) (A.H. Klahn),

[conchi.lopez@qi.ub.es](mailto:conchi.lopez@qi.ub.es) (C. López).

<sup>1</sup> Equal contribution.

**ABSTRACT:**

The synthesis of novel cyrhetrenyl hydrazones of general formula  $[\text{Re}\{\eta^5\text{-C}_5\text{H}_4\text{eC(R}_1\text{)}\frac{1}{4}\text{NNHR}_2\}(\text{CO})_3]$  {with  $\text{R}_1\frac{1}{4}\text{H}$  and  $\text{R}_2\frac{1}{4}\text{4-NO}_2\text{C}_6\text{H}_4$  (4a),  $\text{C}_6\text{H}_5$  (4b) or  $\text{H}$  (4c) or  $\text{R}_1\frac{1}{4}\text{Me}$  and  $\text{R}_2\frac{1}{4}\text{4-NO}_2\text{C}_6\text{H}_4$  (5a),  $\text{C}_6\text{H}_5$  (5b) or  $\text{H}$  (5c)} is described. Compounds 4a and 5a were characterized by mass spectrometry and IR spectroscopy.  $^1\text{H}$  and  $^{13}\text{C}\{^1\text{H}\}$  NMR studies revealed that 4a and 5a adopt the anti-(E) configuration in solution. X-ray crystal structures of compounds 4a and 5c confirmed the transarrangement of the cyrhetrenyl “ $\text{Re}(\eta^5\text{-C}_5\text{H}_4)(\text{CO})_3$ ” and the -NHR<sub>2</sub> moieties and the existence of strong hydrogen bonds involving the eNHe unit. Molecular Orbital calculations at a DFT level have also been carried out in order to rationalize the influence of the nature of the substituent R<sub>3</sub> of  $[\text{R}_3\text{CH}\frac{1}{4}\text{NNH(4-NO}_2\text{C}_6\text{H}_4)]$  ( $\text{R}_3\frac{1}{4}$  ferrocenyl, (3a), cyrhetrenyl (4a), phenyl (6a) or cymantrenyl (7a) on the electronic delocalization, the nucleophilicity of the imine carbon, the polarizability and hyperpolarizability of these compounds, and computational studies using time-dependent density functional (TD-DFT) calculations have also been carried out in order to assign the bands detected in their electronic spectra and to explain the effect produced by the solvent.

## 1. INTRODUCTION

Sandwiches and three legged half-sandwich organometallic compounds have been studied since long ago, but nowadays constitute a very attractive area of research [1e4]. Compounds of this kind with additional  $\text{eC(R1)} \frac{1}{4} \text{Ne}$  or  $\text{eC(R1)} \frac{1}{4} \text{NNHR2}$  groups attached to the rings are specially relevant for different reasons. These include their utility as precursors in organic, inorganic and organometallic synthesis (especially as metallo-ligands to achieve polymetallic derivatives), their interesting (chemical, photochemical, electrochemical) properties as well as their applications in a variety of fields [1e4]. For instance, ferrocenylimines [5,6], oximes [7], azines and azoderivatives [8], thiosemicarbazones [9] or, to a lesser extent, monohydrazones  $[\text{Fe}(\text{h5-C5H5})\{(\text{h5-C5H4}) \text{eC(R1)} \frac{1}{4} \text{NeNHR2}\} (\text{R1} \frac{1}{4} \text{H (1) or Me (2), Fig. 1) or the 1,10-dihydrazones (3) [10,11], are valuable as ligands in coordination and organometallic chemistry (i.e. to achieve cyclometallated compounds) [5,10]. Furthermore, mono- and disubstituted ferrocenyl hydrazones (1e3 in Fig. 1) with large non-linear optical (NLO) properties have also been reported [12].$

On the other hand, the chemistry of cyrhetrene,  $[\text{Re}(\text{h5-C5H5})(\text{CO})_3]$  (the typical example of a three legged half-sandwich rhenium complex), has undergone a rapid development in the last decade [13e15]. Functionalization of the ring or exchange of the CO groups by other mono or bidentate ligands have allowed to prepare a variety of new cyrhetrene derivatives. Most of them exhibit interesting properties, reactivity, (i.e. as metallo-ligands) and biological or catalytic activity [13e15]. Cyrhetrenylimines [6,14], amines [14a] and thiosemicarbazones [9a] have been described in the late years and their properties, applications and activities have been compared with those of their corresponding ferrocenyl analogues [6e9].

Despite the spectacular progress on the design and development of: a) organometallic compounds containing redox active centres [1-4,5a,5b] and b) new hydrazones as stimuli responsive molecules [16], cyrhetrenyl derivatives of the type  $[\text{Re}\{(\text{h5-C5H4}) \text{C(R1)} \frac{1}{4} \text{NNHR2}\}(\text{CO})_3]$  are extremely scarce; as far as we know, that shown in Fig. 1, is the sole example [17]. Moreover, unsubstituted  $[\text{Re}\{(\text{h5-C5H4})\text{eC(R1)} \frac{1}{4} \text{NNH2}\}(\text{CO})_3]$  compounds still remain unknown. In view of this and our interest to compare electronic effects of cyrhetrenyl and ferrocenyl moiety [5-7a,9a,10-11,14,15], here we present six new cyrhetrene derivatives of general formula  $[\text{Re}\{(\text{h5-C5H4})\text{eC(R1)} \frac{1}{4} \text{NNHR2}\}(\text{CO})_3]$  with  $\text{R1} \frac{1}{4} \text{H (4) or Me (5) and R2} \frac{1}{4} 4\text{-NO}_2\text{C}_6\text{H}_4 \text{ (a), C}_6\text{H}_5 \text{ (b) or H(c). It should be noted that those with phenyl rings (4ae4b and 5ae5b) could be visualized as derived from compounds 1 and 2, respectively (Fig. 1) by replacement of the “Fe(h5-C5H5)” unit by the “Re(CO)3” moiety.$

## 2. RESULTS AND DISCUSSION

### 2.1. Synthesis and solution studies

The new cyrhetrenyl hydrazones  $[\text{Re}\{(\text{h}5\text{-C}5\text{H}4)\text{eC}(\text{R}1)\frac{1}{4}\text{NeNHR}2\}(\text{CO})_3]$  (4a, 4b, 5a and 5b) were prepared by adaptation of the procedures reported for their ferrocenyl analogues (1 or 2 in Fig. 1) [12a]; while compounds 4c and 5c (with  $\text{R}2\frac{1}{4}\text{H}$ ) were obtained following the method described for 1,10-diacetylferrocene dihydrazone [10c]. In all cases, the processes are based on condensation reactions between formyl- (for 4ae4c) or acetyl- (for 5ae5c) cyrhetrene and the corresponding hydrazine in anhydrous methanol (Scheme 1). The new compounds, that were isolated as yellow (4ae4c, 5a and 5c) or red (5b) crystalline solids after crystallization from  $\text{CH}_2\text{Cl}_2$ /hexane mixtures, exhibit high solubility in  $\text{CH}_2\text{Cl}_2$  and  $\text{CHCl}_3$ , and they are practically insoluble in hexane. It should be noted that 4c is less stable (in solution as well as in the solid state) than 4a, 4b and 5ae5c and it was characterized immediately after its isolation.

Compounds 4ae4c and 5ae5c were characterized by electron impact (EI) mass spectrometry, infrared spectroscopy and NMR studies. Their MS spectra showed peaks due to the molecular cations  $[\text{M}]^+$  and those arising from the successive dissociation of the remaining CO ligands. IR spectra of 4ae4c and 5ae5c in  $\text{CH}_2\text{Cl}_2$  showed the following common features: a) two intense bands at 2023 and 1929  $\text{cm}^{-1}$ , that are characteristic of the asymmetric (nas) and symmetric (ns) stretchings of the terminal CO ligands of cyrhetrene derivatives [9a,14,15], and b) an intense and sharp absorption (at around 1600  $\text{cm}^{-1}$ ) in the same range as observed for ferrocenyl hydrazones  $[\text{Fe}(\text{h}5\text{-C}5\text{H}5)\{(\text{h}5\text{-C}5\text{H}4)\text{eC}(\text{R}1)\frac{1}{4}\text{NeNHR}2\}]$  with  $\text{R}1\frac{1}{4}\text{H}$  (1) or Me (2) [10e12], that has been assigned to the stretching of the functional  $>\text{C}=\text{N}$ . It is well-known that hydrazones may adopt two different forms (E- or Z-) [6,18] in the solid state and also in solution.  $^1\text{H}$  and  $^{13}\text{C}\{^1\text{H}\}$  NMR spectra of 4ae4c and 5ae5c showed only one set of resonances, thus suggesting that only one of the two isomers was present in  $\text{CDCl}_3$  solution at room temperature (we will return to this point later on).

Proton-NMR spectra of 4ae4c and 5ae5c showed two triplets of identical intensities assigned to the pairs of protons (H2, H5) and (H3, H4) of the “ $\text{Re}(\text{h}5\text{-C}5\text{H}4)$ ” moiety and an additional singlet, in the range  $7.3 < \delta < 8.0$  ppm for 4ae4c, or at around 1.9 ppm (for 5ae5c), due to the  $^1\text{H}$  nuclei of the R1 units (H and Me, respectively). The resonance of the eNHe proton appeared as a broad singlet for 4c and 5c (at 5.26 and 5.48 ppm); while for 4a, 4b, 5a and 5b this signal was much narrower and low-field shifted. Additional resonances due to the aromatic protons of the phenyl rings of 4aeb and 5aeb were also observed.

Comparison of  $^1\text{H}$  NMR data of compounds 4a and 4b and those of their analogues:  $[\text{Fe}(\text{h}5\text{-C}5\text{H}5)\{(\text{h}5\text{-C}5\text{H}4)\text{eC}(\text{H})\frac{1}{4}\text{NeNHR}2\}]$  with  $\text{R}2\frac{1}{4}4\text{-NO}_2\text{C}_6\text{H}_4$  (1a) or  $\text{C}_6\text{H}_5$  (1b) [10a,b] reveal that the replacement of the ferrocenyl unit in 1a (or 1b) by the cyrhetrenyl array to give 4a (or 4b) produces an upfield shift of ca. 0.25 ppm of the singlet due to the eCH]Ne proton; while the resonance eNHe proton

follows the opposite trend [9a]. Thus suggesting that the nature of the organometallic framework modifies the degree of electronic delocalization on the “eC(R1)  $\frac{1}{4}$  NeNH(R2)” unit.  $^{13}\text{C}\{^1\text{H}\}$  NMR spectra of 4a and 5a exhibited the following common signals: a) two singlets in the low field area, of which that at  $\delta$  194 ppm, is due to the terminal CO ligands, and the other to imine carbon, and b) a set of three resonances, two of them in the range  $81 < \delta < 87$  ppm that correspond to the pairs (C2,C5) and (C3,C4) of the C<sub>5</sub>H<sub>4</sub> unit, while the third one that appeared at lower-fields and exhibited lower intensity, is attributed to the C1 carbon atom. For compounds 5a and 5b the resonance of the methylic protons occurred at higher fields and for 4a, 4b, 5a and 5b the group of resonances between 110 and 145 ppm were assigned to the phenyl rings.

As mentioned in previous section with reference to the presence only one of two isomers, the [1H-1H]-NOESY experiments were performed in CDCl<sub>3</sub> at 298 K. In the spectra of 4a and 5a (Figs. S1 and S2) moderate cross-peaks were observed between the amine-NH region ( $\delta$  7.98 for 4a,  $\delta$  7.66 for 5a) and the resonances the protons of the R1 unit ( $\delta$  7.45 for 4a,  $\delta$  2.02 for 5a). This is only possible if the cyrhetrenyl and the eNHR2 groups are in a transarrangement (E-form). Since NMR studies revealed that compounds 4b, 4c, 5b and 5c showed a similar behaviour in solution, we assumed that they also adopted the E form. Compounds 4a and 5c were also characterized by X-ray diffraction.

## 2.2. Description of the crystal structures of compounds 4a and 5c

These structures consist on discrete molecules of  $[\text{Re}\{(\eta^5\text{-C}_5\text{H}_4)\text{eC(R1)}\frac{1}{4}\text{NeNH(R2)}\}(\text{CO})_3]$  {with R1  $\frac{1}{4}$  H and R2  $\frac{1}{4}$  4-NO<sub>2</sub>C<sub>6</sub>H<sub>4</sub> (in 4a) or R1  $\frac{1}{4}$  Me and R2  $\frac{1}{4}$  H (in 5c)} with the typical three-legged piano-stool structure (Figs. 2 and 3, respectively). In the two cases bond lengths and angles of the cyrhetrenyl array as well as the distance Re–centroid of the “C<sub>5</sub>H<sub>4</sub>” ring {hereinafter referred to as Cg(1)} (Table 1) are similar to those reported for related  $[\text{Re}\{(\eta^5\text{-C}_5\text{H}_4\text{R}_3\}\text{(CO)}_3]$  derivatives [14,15,19]. As shown in Figs. 2 and 3, the -NHR2 moiety and the ( $\eta^5$ -C<sub>5</sub>H<sub>4</sub>) unit are in a trans-arrangement [torsion angles: N2eN1eC6eC5  $\frac{1}{4}$  177.1(6)° (in 4a) and N2eN1eC9eC8  $\frac{1}{4}$  179.1(4)° (in 5c)], thus confirming that they also adopt the E form in the solid state.

In 4a, the N1eN2 bond distance [1.368(6) Å] is very similar to that reported for R<sub>3</sub>CH  $\frac{1}{4}$  NeNH(4eNO<sub>2</sub>C<sub>6</sub>H<sub>4</sub>) with R<sub>3</sub>  $\frac{1}{4}$  Ph (6a) [20] [1.361(7) Å], but in 4a the C6eN1 bond length [1.261(7) Å] is shorter than in 6a [1.286(7) Å], thus suggesting that in 4a the >C] Ne bond is stronger than in 6a. Furthermore, the planes defined by the C<sub>5</sub>H<sub>4</sub> (in 4a) ring and the “C5, C6 and N1” form an angle of 4.7° (in 4a); while in 6a the phenyl and the CipsoeC]Ne atoms are less coplanar [interplanar angle  $\frac{1}{4}$  7.8° (in 6a)]. It is well known that for hydrazones R<sub>1</sub>CH  $\frac{1}{4}$  N-NHR2 large angles between main planes of aromatic (or heteroaromatic) groups of the R1 and R2 substituents are usually accompanied with large hyperpolarizabilities, which is relevant in view of their potential non-linear optical properties [16,21]. In PhCH  $\frac{1}{4}$  NeNH(4-NO<sub>2</sub>C<sub>6</sub>H<sub>4</sub>) (6a) this angle (12.5°) is slightly greater than in 4a (11.0°) and, thus the cyrhetrenyl array is expected to produce a decrease in the hyperpolarizability in relation to that of 6a. In compound  $[\text{Re}\{(\eta^5\text{-C}_5\text{H}_4)\text{eC(Me)}\frac{1}{4}\text{NeNH}_2\}(\text{CO})_3]$  (5c): a) the N1eN2 bond length is

practically identical to that of 4a, b) the two bonds of the “Cipso-C=N” unit are a bit larger than in 4a and, c) the imine unit is less co-planar with the C<sub>5</sub>H<sub>4</sub> ring than in 4a [interplanar angles being: 17.9° (in 5c) versus 4.7° (in 4a)]. These findings, that are similar to those found in the ferrocenyylimines [Fe(h<sub>5</sub>-C<sub>5</sub>H<sub>5</sub>){(h<sub>5</sub>-C<sub>5</sub>H<sub>4</sub>)eC(R<sub>4</sub>) ¼ N(C<sub>6</sub>H<sub>5</sub>)] {R<sub>4</sub> ¼ Me or H} [22], suggest that in 4a the electronic communication between the -NHR<sub>2</sub> unit and the cyrhetrenyl array is greater than in 5c (we will return to this point later on). The assembly of the molecules of 4a and 5c in the crystals are markedly different. Figs. S3 and S4 (Supplementary Materials) contain schematic views of the connectivity showing the main intermolecular contacts.

### 2.3. The study of the influence of the R<sub>3</sub> substituent of R<sub>3</sub>CH ¼ NeNH(4-NO<sub>2</sub>C<sub>6</sub>H<sub>4</sub>) and the solvent on their electronic spectra

In a first attempt to elucidate the effect produced by the substituent R<sub>3</sub> on the properties of the hydrazones we decided to perform a comparative study of the ultraviolet-visible spectra of compounds R<sub>3</sub>CH ¼ NeNH(4-NO<sub>2</sub>C<sub>6</sub>H<sub>4</sub>) with R<sub>3</sub> ¼ ferrocenyl (3a), cyrhetrenyl (4a) and phenyl (6a). Absorption spectra of CHCl<sub>3</sub> solutions of 3a, 4a and 6a in CHCl<sub>3</sub> at 298 K (Table 2 and Fig. 4) showed an intense band in the range 380–400 nm. Comparison of data reveals that the replacement of the ferrocenyl unit (in 3a) by the cyrhetrenyl (in 4a) or the phenyl (in 6a) produces a shift of the band to lower wavelengths. The UV-vis spectra of these products in the polar solvents acetone and acetonitrile were practically identical to those obtained in CHCl<sub>3</sub> except for a tiny shift of the band (ca. 5–10 nm) (Table 2 and Figs S5–S7). Computational studies (see below) have allowed us to explain these experimental findings and the origin of this transition. It should be noted that the additional and weaker band observed in the UV-vis. Spectra of 3a in CHCl<sub>3</sub>, acetone or acetonitrile that appears as a shoulder at around 495 nm (Fig. 4 and Fig. S5), is typical of most ferrocene derivatives.

### 2.4. Computational studies on the influence of the R<sub>3</sub> substituent of R<sub>3</sub>CH ¼ NeNH(4-NO<sub>2</sub>C<sub>6</sub>H<sub>4</sub>) on the properties of the compounds

It is well-known that hydrazones are valuable reagents in synthetic chemistry. In this field most of the reactions involve the imine carbon and its nucleophilicity [16,18]. In view of this and in order to compare the effect produced by the substituents R<sub>3</sub> (ferrocenyl, cyrhetrenyl or phenyl) of R<sub>3</sub>CH ¼ NeNH(4-NO<sub>2</sub>C<sub>6</sub>H<sub>4</sub>) on: a) the nucleophilicity of the imine carbon, b) the electronic delocalization between the R<sub>3</sub> substituent and the 4-nitrophenyl ring and, c) the properties of these compounds, we also undertook DFT calculations of hydrazones 3a, 4a and 6a. For comparison purposes the cymantrene derivative (7a) with R<sub>3</sub> ¼ Mn(h<sub>5</sub>-C<sub>5</sub>H<sub>4</sub>)(CO)<sub>3</sub> was also included.

All the calculations were carried out using the B3LYP hybrid functional [24] and the LANL2DZ basis set [25] implemented in the Gaussian09 program [26]. Geometries of compounds 3a, 4a and 7a were optimised without imposing any restriction. Final atomic coordinates for the optimized geometries are included as supplementary information, (Tables S1–S4). Bond lengths and angles of the optimised

geometry of 4a and 6a were consistent with those obtained from the X-ray studies (the differences did not clearly exceed 3s) and those of 3a fall in the range reported for related ferrocenyl Schiff bases [19]. Afterwards, molecular orbital (MO) calculations of the optimized geometries were carried out. Comparison of the calculated HOMO - LUMO energy gaps ( $E_{\text{LUMO}} - E_{\text{HOMO}}$ ) (Table S5) reveals that DE increases as follows:  $3a < 6a < 4a \leq 7a$ . Thus showing that the ferrocenyl (in 3a) or the "M(h5-C5H4)(CO)3" unit (in 4a and 7a) produce opposite effects on the energy gap when compared the phenyl derivative (6a).

As shown in Fig. 5 for the four compounds HOMO (and also LUMO) are similar; however, a careful analysis of their compositions reveal significant variations in the contributions of the main fragments [R3, eCH]NeNHe and the 4-nitrophenyl group (Table S5). For 4a, 6a and 7a, the contributions of the 4-nitrophenyl group and the R3 substituent are very similar, but in 6a the hydrazone has a greater contribution than in 4a and 7a. For 3a, the relative weight of the nitrophenyl (18%) groups is significantly smaller than in 4a, 7a and 6a, and the participation of ferrocenyl group reaches the 47%. A parallel situation arises from the comparison of the LUMO orbitals, for 3a the contribution of the 4-NO2C6H4 (82%) is higher than in 4a, 6a and 7a (Table S5).

Comparative analyses of the charge distribution on the 4-nitrophenyl group, shows that the ferrocene derivative (3a) concentrates electron density (that is, larger negative charge) in the eNO2 group (Table S6), but it decreases for 4a, 6a and 7a derivatives. In addition, the charge of the imine carbon increases according to the trend  $4a \leq 6a \leq 7a < 3a$ . This finding indicates the replacement of the cyrhetrenyl, cymantrenyl or phenyl groups by a ferrocenyl unit produces a significant change in the nucleophilicity of this carbon which is relevant in view of their reactivity and potential utility in synthesis [16,18].

As mentioned above, it is well-known that hydrazones are also attractive to achieve non linear optic (NLO) systems [12,16,18,21]. In these cases, the analysis of the effect of an external electric field on the permanent dipole moment is a valuable tool to understand their potential NLO properties. When small modification of the dipole moment is expected, a linear model considering the polarizability is used, which is equivalent to apply the harmonic approximation. Since the nature of the NLO response follows from the periodic vibration, we have also calculated static ( $\alpha(0)$ ) and frequency-dependent ( $\alpha(\omega)$ ) vacuum polarizabilities of the four hydrazones. The results (Table S7), reveal that isotropic polarizabilities increase according to the sequence  $6a < 3a < 7a < 4a$ .

On the other hand, the inclusion of an anharmonic correction related to the second order term allows the determination of the hyperpolarizability, a third order tensor divided into tensorial components. A strong hyperpolarizability results in a large second order NLO response. According to our calculations (Table S8), hyperpolarizabilities are higher in the plane containing the aromatic rings. This fact can be ascribed to the easier flow of electrons along the p system. Also, changes in the substituent R3 result in significant variations of the hyperpolarizability. In particular, for compounds 3a, 4a and 7a, where the imine carbon is attached to the C5H4 ring, the first hyperpolarizability follows the trend  $6a < 7a \ll 3a$ . This is consistent with the differences in the relative orientation of the rings (Table S9). The non-

planarity of the aromatic system results in a breakage of the p system that lowers the hyperpolarizability. On these basis, compound 3a, appears to be the best candidate for a large NLO response. On the other hand and in order to elucidate the origin of the intense band detected in the UVevis spectra of compounds 3a, 4a and 6a in the range 380 nm-410 nm, we decided to undertake a study based on the time-dependent DFT (TD-DFT) methodology [27] to achieve the assignment of the bands detected in the UVevis. spectra of hydrazones 3a, 4a and 6a. For comparison purposes, we also included compound 7a. After the optimization of the geometries (see above), the excitation energies and the corresponding oscillator strengths were calculated. The results obtained from calculations in gas phase, CHCl<sub>3</sub> and acetone reveal that the absorption band at around 400 nm arises from a combination of several transitions, of which those with greater contribution are presented in Table 3. For compounds 4a and 6a, the main contribution arises from HOMO / LUMO transition (Table 3 and Fig. 5); but for 3a and 7a, the observed band results from the combination of several transitions. One of them is the HOMO/LUMO, but now its relative weight is clearly smaller than for 4a and 6a. Additional transitions occurring in the same energy range, but with smaller contributions than are presented in Table 3. These studies also revealed that when CHCl<sub>3</sub> is replaced by acetone the band shifts to higher wavelengths (Fig. S8 Table S10) in good agreement with the experimental results (Table 2). The computational analysis of the results obtained for 3a also confirmed the existence of a d-d transition of the Fe (II) centre at ca. 495-500 nm that agrees with the shoulder observed in the UVevis. spectra of compound 3a (Fig. 4 and Fig. S5).



### 3. CONCLUSIONS

We have prepared and characterized six novel cyrhetrenyl hydrazones  $[\text{Re}\{(\eta^5\text{-C}_5\text{H}_4)\text{eC}(\text{R}_1)\frac{1}{4}\text{NNHR}_2\}(\text{CO})_3]$   $\{\text{R}_1\frac{1}{4}\text{H}$  (4) or Me (5) and  $\text{R}_2\frac{1}{4}\text{4-NO}_2\text{C}_6\text{H}_4$  (a),  $\text{C}_6\text{H}_5$  (b) or H (c) $\}$ . NMR studies and the crystal structures of 4a and 5c confirm that the organometallic framework and the amine nitrogen are in a trans-arrangement (Eform). It should be noted that Re(I) compounds similar to those presented here were not known before, except for  $[\text{Re}\{(\eta^5\text{-C}_5\text{H}_4)\text{eCH}\}\text{NNH}[(2,4\text{-NO}_2)_2\text{C}_6\text{H}_3]\}(\text{CO})_3]$  (Fig. 1) that was described in 1981. Moreover, the comparison of the results obtained from theoretical studies undertaken for hydrazones  $[\text{R}_3\text{CH}\frac{1}{4}\text{NNH}(4\text{-NO}_2\text{C}_6\text{H}_4)]$   $\{\text{with R}_3\frac{1}{4}\text{ferrocenyl}$  (3a), cyrhetrenyl (4a), cymantrenyl (7a) or phenyl (6a) $\}$  have allowed us to explain the effect produced by the  $\text{R}_3$  groups on: a) the HOMO and LUMO orbitals and the energy gap, b) the charge distribution and the nucleophilicity of the imine carbon, and c) their polarizabilities and hiperpolarizabilities.

Computational studies undertaken using TD-DFT methodology reveal a reasonable agreement between the experimental and calculated UV-vis. spectra and have allowed the assignment of the main absorptions and to explain the effect produced by the substituent  $\text{R}_3$  on their absorption spectra in two different solvents ( $\text{CHCl}_3$  and acetone).

## 4. EXPERIMENTAL SECTION

### 4.1. Experimental details

Reactions were performed under a nitrogen atmosphere using standard Schlenk techniques. 4-Nitrophenylhydrazine (98%), phenylhydrazine (98%) and hydrazine monohydrate (65%) were obtained from Aldrich and used as received, and compounds  $[\text{Re}(\eta^5\text{-C}_5\text{H}_4\text{C}(\text{O})\text{R}_1)(\text{CO})_3]$  ( $\text{R}_1 = \text{H}$  or  $\text{Me}$ ) were prepared as described before [14b,c]. Solvents ( $\text{CH}_2\text{Cl}_2$ ,  $\text{MeOH}$ ,  $\text{EtOH}$  and hexane) were obtained from commercial sources and purified following standard methods [28]. Electron impact (EI) mass spectrawere obtained on a Shimadzu GC-MS spectrometer (70 eV) at the Laboratorio de Servicios Analíticos, (Pontificia Universidad Católica de Valparaíso). Infrared spectra were recorded in  $\text{CH}_2\text{Cl}_2$  solution using NaCl cells and a PerkinElmer - 1605 FT-IR spectrophotometer. Ultraviolet-visible spectra of compounds 3a, 4a and 6a in  $\text{CHCl}_3$  (99.4%); acetone (99.5%) or acetonitrile (99.9%) were recorded at 298 K with a SHIMADZU UV-1800 spectrophotometer.  $^1\text{H}$  and  $^{13}\text{C}\{^1\text{H}\}$  NMR spectra were registered at 298 K on a Bruker AVANCE 400 III and Bruker Fourier 300 spectrometers using  $\text{CDCl}_3$  as a solvent. The chemical shifts are referenced to the residual deuterated solvent peaks. Chemical shifts ( $\delta$ ) are given in ppm, and the coupling constants ( $J$ ) in Hz. In the characterization section of compounds 4a and 5a the assignment of NMR data correspond to the labelling pattern presented in Scheme 1. [Abbreviations for the multiplicities of the signals detected in  $^1\text{H}$  NMR: s (singlet), d (doublet), t (triplet), m (multiplet) and br.s (broad singlet)].

### 4.2. Synthesis of the compounds

$[\text{Re}\{\eta^5\text{-C}_5\text{H}_4\text{C}(\text{O})\text{R}_1\}(\text{CO})_3]$  with  $\text{R}_1 = \text{H}$  (4a) or  $\text{Me}$  (5a). Hydrazones 4a and 5a were prepared as described for the analogous ferrocenyl hydrazones [12a], except for the following experimental conditions: a) the reactions were performed under  $\text{N}_2$  atmosphere, b) the corresponding  $[\text{Re}\{\eta^5\text{-C}_5\text{H}_4\text{C}(\text{O})\text{R}_1\}(\text{CO})_3]$  derivative [125 mg, 0.34 mmol (for  $\text{R}_1 = \text{H}$ ) or 163 mg, 0.43 mmol (for  $\text{R}_1 = \text{Me}$ )] was treated with the stoichiometric amount of 4-nitrophenylhydrazine and anhydrous ethanol (8 mL) was used as solvent, c) the reaction mixture was stirred for 2 h in the presence of molecular sieves and d) the solid formed after this period was collected by filtration, washed with three portions of 5 mL of cold ethanol and the solvent was removed in a rotary evaporator. Compounds 4a and 5a were isolated as yellow solids. Yields: 62% (105 mg, 0.21 mmol) for 4a and 75% (165 mg, 0.32 mmol) for 5a. Characterization data for 4a: MS (based on  $^{187}\text{Re}$ )  $m/z$ : 499  $[\text{M}]^+$ ; 471  $[\text{M} - \text{CO}]^+$ ; 443  $[\text{M} - 2\text{CO}]^+$  and 415  $[\text{M} - 3\text{CO}]^+$ ; IR data ( $\text{CH}_2\text{Cl}_2$ ,  $\text{cm}^{-1}$ ): 2025 (s)  $\nu(\text{CO})$ ; 1930 (vs),  $\nu(\text{CO})$  and 1598 (w),  $\nu(>\text{C})\text{Ne}$ .  $^1\text{H}$  NMR data (400 MHz,  $\text{CDCl}_3$ ):  $\delta$  5.40 (t, 2H,  $^3J_{\text{H,H}} = 2.3$ ,  $\text{H}_3$  and  $\text{H}_4$ ); 5.82 (t, 2H,  $^3J_{\text{H,H}} = 2.3$ ,  $\text{H}_2$  and  $\text{H}_5$ ); 7.04 (d, 2H,  $^3J_{\text{H,H}} = 8.2$ , 2H<sub>b</sub>); 7.45 (s, 1H, eCH<sub>3</sub>Ne); 7.98 (s, 1H, eNHe) and 8.17 (d, 2H,  $^3J_{\text{H,H}} = 8.2$ , 2H<sub>a</sub>).  $^{13}\text{C}\{^1\text{H}\}$  NMR data ( $\text{CDCl}_3$ ):  $\delta$  84.9 (C2 and C5); 85.6 (C3 and C4); 102.1 (C1); 113.2 (C<sub>a</sub>); 127.4 (C<sub>b</sub>); 134.1 (C<sub>g</sub>); 150.0 ( $>\text{C}$ )Ne, 194.4 (CO) the

resonance due to the quaternary Cipso carbon was not observed. For 5a: MS (based on  $^{187}\text{Re}$ )  $m/z$ : 513  
 [M] $^+$ ; 485 [M - CO] $^+$ ; 457 [M - 2CO] $^+$  and 429 [M - 3CO] $^+$ ; IR data ( $\text{CH}_2\text{Cl}_2$ ,  $\text{cm}^{-1}$ ): 2024 (s),  
 n(CO); 1929 (vs), n(CO) and 1601 (w), n(>C]Ne).  $^1\text{H}$  NMR data (300 MHz,  $\text{CDCl}_3$ ):  $\delta$  2.02 (s, 3H,  
 Me); 5.39 (t, 2H, 3JH,H  $\frac{1}{4}$  2.3, H3 and H4); 5.82 (t, 2H, 3JH,H  $\frac{1}{4}$  2.3, H2 and H5); 7.10 (d, 2H, 3JH,H  
 $\frac{1}{4}$  8.2, 2Hb); 7.66 (s, 1H, eNHe) and 8.18 (d, 2H, 3JH,H  $\frac{1}{4}$  8.2, 2Ha).  $^{13}\text{C}\{^1\text{H}\}$  NMR data ( $\text{CDCl}_3$ ):  $\delta$   
 31.6 (Me); 82.9 (C2 and C5); 84.4 (C3 and C4); 104.4 (C1); 112.3 (Ca); 126.1 (Cb); 138.7 (Cg); 140.9  
 (Cipso); 149.1 (>C]Ne) and 193.4 (CO).  
 [Re{(h5-C5H4)eC(R1)  $\frac{1}{4}$  NeNH(C6H5))}(CO) $_3$ ] with R1  $\frac{1}{4}$  H (4b) or Me (5b). The synthesis of these  
 products was carried out following the same procedure as described above for 4a and 5a, [Re{(h5-  
 C5H4C(O)R1)}(CO) $_3$ ] derivative [100 mg, 0.275 mmol (for R1  $\frac{1}{4}$  H) or 100 mg, 0.28 mmol (for R1  $\frac{1}{4}$   
 Me)], but replacing the 4- nitrophenylhydrazine by the stoichiometric amount of phenylhydrazine [27.2  
 mL, (0.275 mmol) and 27.7 mL, (0.28 mmol) for 4b and 5b, respectively]. After work-up, the desired  
 compounds were isolated as yellow (4b) and red (5b) solids. These products were afterwards  
 recrystallized in a  $\text{CH}_2\text{Cl}_2$ /hexane (1:5) mixture at  $-18 \pm 1^\circ\text{C}$ . Yields: 78% (95 mg, 0.21 mmol) for 4b,  
 and 86% (110 mg, 0.24 mmol) for 5b. Characterization data for 4b: MS (based on  $^{187}\text{Re}$ )  $m/z$ : 454  
 [M] $^+$ ; 426 [M - CO] $^+$ ; 398 [M - 2CO] $^+$  and 370 [M - 3CO] $^+$ ; IR data ( $\text{CH}_2\text{Cl}_2$ ,  $\text{cm}^{-1}$ ): 2024 (s),  
 n(CO); 1929 (vs), n(CO) and 1599 (w), n(>C]Ne).  $^1\text{H}$  NMR data (400 MHz,  $\text{CDCl}_3$ ):  $\delta$  5.34 (t, 2H,  
 3JH,H  $\frac{1}{4}$  2.3, H3 and H4); 5.75 (t, 2H, 3JH,H  $\frac{1}{4}$  2.3, H2 and H5); 6.84 (m, 3H, 2Hb and Hg); 7.02 (m,  
 2H, 2Ha); 7.37 (s, 1H, eCH] Ne) and 7.56 (s, 1H, eNHe).  $^{13}\text{C}\{^1\text{H}\}$  NMR data ( $\text{CDCl}_3$ ):  $\delta$  82.5 (C2 and  
 C5); 83.9 (C3 and C4); 102.4 (C1); 112.9 (Ca); 120.7 (Cg); 128.2 (Cipso); 129.3 (Cb); 143.9 (eCH]Ne)  
 and 193.7 (CO). For 5b: MS (based on  $^{187}\text{Re}$ )  $m/z$ : 468 [M] $^+$ ; 440 [M - CO] $^+$ ; 412 [M - 2CO] $^+$  and  
 384 [M - 3CO] $^+$ ; IR data ( $\text{CH}_2\text{Cl}_2$ ,  $\text{cm}^{-1}$ ): 2022 (s), n(CO); 1924 (vs), n(CO) and 1597 (w),  
 n(>C]Ne).  $^1\text{H}$  NMR data (400 MHz,  $\text{CDCl}_3$ ):  $\delta$  1.97 (s, 3H, Me); 5.35 (t, 2H, 3JH,H  $\frac{1}{4}$  2.3, H3 and H4);  
 5.75 (t, 2H, 3JH,H  $\frac{1}{4}$  2.3, H2 and H5); 6.87 (m, 3H, 2Hb and Hg); 7.09 (m, 2H, 2Ha); and 7.25 (s, 1H,  
 eNHe).  $^{13}\text{C}\{^1\text{H}\}$  NMR data ( $\text{CDCl}_3$ ):  $\delta$  30.1 (Me); 81.9 (C2 and C5); 84.0 (C3 and C4); 101.8 (C1);  
 113.4 (Ca); 120.5 (Cg); 129.4 (Cb); 144.5 (>C]Ne) and 194.0 (CO); the resonance due to the quaternary  
 Cipso carbon was not observed.  
 [Re{(h5-C5H4)eC(R1)  $\frac{1}{4}$  NeNH $_2$ )}(CO) $_3$ ] with R1  $\frac{1}{4}$  H (4c) or Me (5c). The corresponding [Re(h5-  
 C5H4C(O)R1)(CO) $_3$ ] compound {with R1  $\frac{1}{4}$  H (100 mg, 0.27 mmol) (for 4c) or Me (100 mg; 0.26  
 mmol) (for 5c)} was dissolved in anhydrous methanol (12 mL) and treated with an excess of hydrazine  
 monohydrate (140 mL, 2.7 mmol). The reaction mixture was stirred under  $\text{N}_2$  atmosphere for 2 h (for  
 4c) or 18 h (for 5c). Then, the solvent was evaporated to dryness under vacuum. The residue was  
 dissolved in 10 mL of  $\text{CH}_2\text{Cl}_2$ , transferred to an extraction funnel, and treated with 30 mL of water to  
 remove the excess of hydrazine. Finally, the organic extract was collected, dried over  $\text{Na}_2\text{SO}_4$  and  
 solution was concentrated to dryness on a rotary evaporator giving yellow solids. They were later on  
 recrystallized in  $\text{CH}_2\text{Cl}_2$ /hexane mixtures [(1:5) (for 4c) or (1:3) (for 5c)] at  $-18 \pm 1^\circ\text{C}$ . (Yields: 69% (70  
 mg, 0.19 mmol) for 4c and 69% (70 mg, 0.18 mmol) for 5c. Characterization data for 4c: MS (based on

187Re) m/z: 378 [M]<sup>+</sup>; 350 [M - CO]<sup>+</sup>; 322 [M - 2CO]<sup>+</sup> and 294 [M - 3CO]<sup>+</sup>; IR data (CH<sub>2</sub>Cl<sub>2</sub>, cm<sup>-1</sup>): 2024 (s), n(CO); 1920 (vs), n(CO); 1603 (w), n(>C]Ne). <sup>1</sup>H NMR data (400 MHz, CDCl<sub>3</sub>): δ 5.31 (t, 2H, 3JH,H ¼ 2.3, H3 and H4); 5.48 (br.s, 2H, NH<sub>2</sub>); 5.66 (t, 2H, 3JH,H ¼ 2.3, H2 and H5); 7.34 (s, 1H, eCH]Ne). <sup>13</sup>C{<sup>1</sup>H} NMR data (CDCl<sub>3</sub>): δ 84.8 (C2 and C5); 86.4 (C32 and C4); 95.8 (C1); 154.8 (eCH]Ne) and 192.5 (CO). For 5c: MS (based on 187Re) m/z: 392 [M]<sup>+</sup>; 364 [M - CO]<sup>+</sup>; 336 [M - 2CO]<sup>+</sup>; 308 [M - 3CO]<sup>+</sup>; IR data (CH<sub>2</sub>Cl<sub>2</sub>, cm<sup>-1</sup>): 2021 (s), n(CO); 1925 (vs), n(CO) and 1608 (w), n(>C]Ne). <sup>1</sup>H NMR data (400 MHz, CDCl<sub>3</sub>): δ 1.86 (s, 3H, Me); 5.26 (br.s, 2H, NH<sub>2</sub>); 5.32 (t, 2H, 3JH,H ¼ 2.3, H3 and H4); 5.66 (t, 2H, 3JH,H ¼ 2.3, H2 and H5). <sup>13</sup>C{<sup>1</sup>H} NMR data (CDCl<sub>3</sub>): δ 12.2 (Me); 81.9 (C2 and C5); 84.0 (C3 and C4); 106.8 (C1); 139.7 (>C]Ne) and 193.9 (CO).

### 4.3. Crystal structure determinations

A prismatic crystal of 4a or 5c (sizes in Table 4) was selected. The former was mounted on a MAR345 diffractometer with an image plate detector. Unit-cell parameters (Table 4) were determined from 255 reflections ( $3^\circ < 2\theta < 31^\circ$ ) and refined by least-squares method. Intensities were collected with graphite monochromatized Mo K $\alpha$  radiation.

For 4a, 11801 reflections were measured in the range  $1.78^\circ \leq 2\theta \leq 30.30^\circ$ , of which 3765 were non-equivalent by symmetry { $R_{int}$  (on I) ¼ 0.0488} and 3192 reflections were assumed as observed applying the condition  $I > 2s(I)$ . Lorentz-polarization and absorption corrections were made. The structure was solved by Direct methods, using SHELXS computer program [29] and refined by fullmatrix least-squares method with SHELXL97 computer program [30] using 11801 reflections, (very negative intensities were not assumed). The function minimized was  $\sum w [|F_o|^2 - |F_c|^2]^2$ , where  $w = 1/[s^2(I) + (0.0556P)^2 + 0.5148P]$ ,  $P = (|F_o|^2 + 2|F_c|^2)/3$ ,  $f$ ,  $f_0$  and  $f_{00}$  were taken from International Tables of X-Ray Crystallography [31]. All H atoms were computed and refined, using a riding model, with an isotropic temperature factor equal to 1.2 times the equivalent temperature factor of the atom linked.

The crystal of 5c was mounted on top of glass fibres in a random orientation. Diffraction data were collected at 296.15 K on a Bruker D8 QUEST diffractometer equipped with a bidimensional CMOS Photon100 detector, using graphite monochromated Mo-K $\alpha$  radiation. The diffraction frames were integrated using the APEX2 package [32] and were corrected for absorptions with SADABS. Using OLEX2 as graphical interface, the structure was solved with OLEX2 structure solution program [33] by charge flipping and refined with the Gauss-Newton refinement package. In this case, non-hydrogen atoms were refined with anisotropic displacement parameters and H atoms were finally included in their calculated positions.

The final  $R$  (on  $F$ ) factor was 0.036 for 4a, and 0.015 for 5c;  $wR$  (on  $|F|^2$ ) ¼ 0.098 (4a) [or 0.044 (5c)], and the goodness of fit ¼ 1.141 and 1.396 (for 4a and 5c, respectively). The number of refined parameters and further details concerning the resolution and refinement of the crystal structures of 4a and 5c are presented in Table 4.

#### 4.4. Theoretical studies

Calculations were carried out using the Gaussian09 package [26]. The hybrid density function method known as B3LYP was applied [24]. Effective core potentials (ECP) were used to represent the innermost electrons of the transition metal atom (Fe and Re) and the basis set of valence double-z quality for associated with the pseudopotentials known as LANL2DZ [25]. The basis set for the main group elements was 6-31G\* (C, N, O and H) [34]. All molecular structures were optimized without symmetry constraints and characterized as minima by vibrational analysis. Polarizabilities and hyperpolarizabilities were computed using frequency-dependent ( $\omega = 0.1$  Ha) [35].

## ACKNOWLEDGMENTS

A.H.K. and R.A. acknowledge FONDECYT-Chile (Projects 11130443, 1110669 and 1150601), FONDEQUIP EQM 130154 and D.I. Pontificia Universidad Católica de Valparaíso; J.G. is grateful to the CONICYT for a Doctoral scholarship and D.I.-PUCV and G.A., R.B and C.L acknowledge the financial support from the Dirección General de Investigación (DGI) of Spain (Grants n. CTQ2015-6459-C3-1-P and CTQ2015-65040-P).

## REFERENCES

- [1] a) J.M. O'Connor, in: E.W. Abel, F.G.A. Stone, G. Wilkinson (Eds.), *Comprehensive Organometallic Chemistry II*, Pergamon, Oxford, U.K. 6, 1995, p. 167; b) C. Pettinari, R. Pettinari, C. Di Nicola, F. Marchetti, in: A.J.L. Pombeiro (Ed.), *Advances in Organometallic Chemistry and Catalysis*, 2014, pp. 269e1284.
- [2] a) R. Peters, D.F. Fischer, S. Jautze, *Top. Organomet. Chem.* 33 (2011) 139e175; b) A.S. Abd-El-Aziz, C. Agatemor, N. Etkin, *Macromol. Rapid Commun.* 35 (2014) 513e559; c) G. Kehr, G. Erker, in: I. Marek, Z. Rappoport (Eds.), *Chemistry of Organoiron Compounds*, Wiley, Weinheim, Germany, 2014, pp. 233e247; d) A. Togni, T. Hayashi (Eds.), *Ferrocenes. Homogeneous Catalysis, Organic Synthesis. Materials Science*, VCH, Weinheim, Germany, 1995; e) P. Stepnicka (Ed.), *Ferrocene. Ligands, Materials and Biomolecules*, Wiley, Weinheim, Germany, 2008.
- [3] a) S. Toma, J. Csizmadiova, M. Meciariova, R. Sebesta, *Dalton Trans.* 43 (2014) 16557e16579; b) L. Peng, A. Feng, M. Huo, J. Yuan, *Chem. Commun.* 50 (2014) 13005e13014; c) A.E. Kaifer, *Acc. Chem. Res.* 47 (2014) 2160e2167; d) R. Sun, L. Wang, H. Yu, Z. Abidin, Y. Chen, J. Huang, R. Tong, *Organometallics* 33 (2014) 4560e4573; e) S.S. Braga, A.M.S. Silva, *Organometallics* 32 (2013) 5626e5639; f) M. Senel, *Adv. Chem. Res.* 10 (2011) 393e408.
- [4] For recent and relevant contributions on half-sandwiches compounds see for instance: a) V. Turkey, S. Mishra, H.R. Dash, S. Das, B.P. Nayak, S.M. Mobin, S. Chatterjee, *J. Organomet. Chem.* 732 (2013) 122e129; b) Y.-F. Han, G.-X. Jin, *Acc. Chem. Res.* 47 (2014) 3571e13579; c) Y.-F. Han, G.-X. Jin, *Chem. Soc. Rev.* 43 (2014) 2799e2823; d) S.K. Singh, D. Pandey, S. Daya, *RSC Adv.* 4 (2014) 1819e11840; e) I. Remy, P. Brossier, I. Lavastre, J. Besancon, C. Moise, *J. Pharm. Biomed.* 9 (1991) 965e967; f) X. Wu, J. Xiao, in: P. Dixneuf, V. Cadierno (Eds.), *Metal-catalyzed Reactions in Water*, 2013, pp. 173e242; g) M. Hapke, C.C. Tzschucke, *Angew. Chem. Int. Ed.* 52 (2013) 3317e3319; h) W.E. Geiger, *Coord. Chem. Rev.* 257 (2013) 1459e1471.
- [5] See for instance: a) C. López, R. Bosque, M. Pujol, J. Simó, E. Sevilla, M. Font-Bardía, R. Messeguer, C. Calvis, *Inorganics* 2 (2014) 620e648; b) D. Talancón, C. López, M. Font-Bardía, T. Calvet, O. Roubeau, *Eur. J. Inorg. Chem.* (2014) 213e220; c) R. Cortés, M. Tarrado-Castellarnau, D. Talancón, C. López, W. Link, D. Ruiz, J. Centelles, J. Quirante, M. Cascante, *Metallomics* 6 (2014) 622e633; d) D. Talancón, C. López, M. Font-Bardía, T. Calvet, J. Quirante, C. Calvis, R. Messeguer, R. Cortés, M. Cascante, L. Baldomá, J. Badia, *J. Inorg. Biochem.* 118 (2013) 1e12 and references cited in these articles.
- [6] a) R. Arancibia, A.H. Klahn, G.E. Buono-Cuore, D. Contreras, G. Barriga, C. Olea-Azar, M. Lapier, J.D. Maya, A. Ibañez, M.T. Garland, *J. Organomet. Chem.* 743 (2013) 49e54; b) R. Arancibia, A.H. Klahn, G.E. Buono-Core, E. Gutierrez-Puebla, A. Monge, M.E. Medina, C. Olea-Azar, J.D. Maya, F. Godoy, *J. Organomet. Chem.* 696 (2011) 3228e3244.
- [7] a) C. López, R. Bosque, X. Solans, M. Font-Bardía, *J. Organomet. Chem.* 539 (1997) 99e107; b) H.-M. Li, A.-Q. Feng, X.-H. Lou, *Bull. Korean Chem. Soc.* 35 (2014) 2551e2554.
- [8] a) H. Nishihara, *Bull. Chem. Soc. Jpn.* 77 (2004) 407e428; b) M. Kurihara, H. Nishihara, *Coord. Chem. Rev.* 226 (2002) 125e135; c) A.A. Musikhina, I.A. Utepova, P.O. Serebrennikova, O.N. Chupakhin, V.N. Charushin, *Russ. J. Org. Chem.* 49 (2013) 1191e1194; d) Z.-Q. Hao, J.-F.

- 458 Gong, W.-T. Song, Y.-J. Wu, M.-P. Song, *Inorg. Chem. Commun.* 10 (2007) 371e375; e) R.  
 459 Bosque, C. Ll opez, J. Sales, X. Solans, J. Silver, *J. Chem. Soc. Dalton Trans.* (1996)  
 460 3195e3200; f) A.G. Osborne, M. Webba da Silva, M.B. Hursthouse, K.M.A. Malik, G.  
 461 Opromolla, P. Zanello, *J. Organomet. Chem.* 516 (1996) 167e176.
- 462 [9] a) R. Arancibia, A.H. Klahn, M. Lapier, J.D. Maya, A. Ibañez, M.T. Garland, S. Carrere-  
 463 Kremer, L. Kremer, C. Biot, *J. Organomet. Chem.* 755 (2014) 1e6; b) G. Li, Z. Shi, X. Li, Z.  
 464 Zhigang, *J. Chem. Res.* 35 (2011) 278e281.
- 465 [10] a) C. Ll opez, J. Granell, *J. Organomet. Chem.* 555 (1998) 211e225; b) C. Ll opez, R. Bosque,  
 466 X. Solans, M. Font-Bardía, *J. Organomet. Chem.* 535 (1997) 99e105; c) M.M. Abd-Elzaher,  
 467 W.H. Hegazy, A. El-Din, M. Gaafar, *Appl. Organomet. Chem.* 19 (2005) 911e916; d) N.G.  
 468 Shikhaliyev, A.V. Gurbanov, V.M. Muzalevsky, V.G. Nenajdenkob, V.N. Khrustalev, *Acta*  
 469 *Cryst. E70* (2014) m286em287.
- 470 [11] a) C. Ll opez, R. Bosque, J. Arias, E. Evangelio, X. Solans, M. Font-Bardía, *J. Organomet.*  
 471 *Chem.* 672 (2003) 34e42; b) D. Csokas, I. Zupka, B.I. Karalyi, L. Drahos, T. Holczbauer, A.  
 472 Pallo, M. Czugler, A. Csampi, *J. Organomet. Chem.* 743 (2013) 130e138; c) E.A. Raspopova,  
 473 A.N. Morozov, A.O. Bulanov, L.D. Popov, I.N. Shcherbakov, S.I. Levchenkov, V.A. Kogan,  
 474 *Russ. J. Gen. Chem.* 82 (2012) 1457e1468; d) P. Krishnamoorthy, P. Sathyadevi, R.R. Butorac,  
 475 A.H. Cowley, S.P.N. Bhuvanesh, *Dalton Trans.* 41 (2012) 4423e4438; e) J. Zhang, R. Liu, J.  
 476 *Chem. Soc. Pak.* 33 (2011) 356e359.
- 477 [12] a) A. Houlton, N. Jasim, R.M.G. Roberts, J. Silver, D. Cunningham, P. McArdle, T. Higgins, J.  
 478 *Chem. Soc. Dalton Trans.* (1992) 2235e2241; b) A. Houlton, J.R. Miller, J. Silver, N. Jassim,  
 479 M.J. Ahmet, *Inorg. Chim. Acta* 205 (1993) 67e70; c) M. Fuentealba, L. Toupet, C. Manzur, D.  
 480 Carrillo, I. Ledoux-Rak, J.R. Hamon, *J. Organomet. Chem.* 692 (2007) 1099e1109.
- 481 [13] Recent and relevant contributions on cyrhetrene derivatives: a) I.V. Skabitskii, E.I. Romadina,  
 482 A.A. Pasynskii, Zh V. Dobrokhotova, S.G. Sakharov, *Russ. J. Coord. Chem.* 40 (2014)  
 483 813e820; b) G.A. Koutsantonis, P.L. Low, C.F.R. Mackenzie, B.W. Skelton, D.S. Yufit,  
 484 *Organometallics* 33 (2014) 4911e4922; c) T.S. Teets, J.A. Labinger, J.E. Bercaw,  
 485 *Organometallics* 33 (2014) 4107e4117; d) Q. Nadeem, D. Can, Y. Shen, F. Yunjun, M. Felber,  
 486 Z. Mahmood, R. Alberto, *Org. Biomol. Chem.* 12 (2014) 1966e1974; e) R.D. Young, A.F. Hill,  
 487 G.E. Cavigliasso, R. Stranger, *Angew. Chem. Int. Ed.* 52 (2013) 3699e3702.
- 488 [14] a) R. Arancibia, F. Godoy, G. Buono-Core, A.H. Klahn, E. Gutierrez-Puebla, A. Monge,  
 489 *Polyhedron* 27 (2008) 2421e2425; b) J. Heldt, N. Fischer-Durand, M. Salmay, A. Vessières,  
 490 G. Jaouen, *J. Organomet. Chem.* 689 (2004) 4775e4782; c) S. Jones, M. Rausch, P. Bitterwolf,  
 491 *J. Organomet. Chem.* 396 (1990) 279e287.
- 492 [15] a) D. Sierra, N. Bhuvanesh, J.H. Reibenspies, J.A. Gladysz, A.H. Klahn, *J. Organomet. Chem.*  
 493 749 (2014) 416e420; b) T. Cautivo, H. Klahn, F. Godoy, C. Ll opez, M. Font-Bardía, T. Calvet,  
 494 E. Gutierrez-Puebla, A. Monge, *Organometallics* 30 (2011) 5578e5589.
- 495 [16] L.A. Tatum, X. Su, I. Aprahamian, *Acc. Chem. Res.* 47 (2014) 2141e2149.
- 496 [17] N. Kolobova, Z. Valueva, M. Solodova, *Bull. SSSR Acad. Sci. Div. Chem.* 29 (1981)  
 497 1701e1705.
- 498 [18] D. Barton, W.D. Ollis (Eds.), *Comprehensive Organic Chemistry*, Pergamon, Oxford, U.K.,  
 499 1979.



- 500 [19] a) F.H. Allen, *Acta Cryst. Sect. B Struct. Sci.* B58 (2002) 380e388; b) Cambridge  
501 Crystallographic Data Centre. Available online: [www.ccdc.cam.ac.uk/data\\_request/cif](http://www.ccdc.cam.ac.uk/data_request/cif)  
502 (accessed on 24.07.15).
- 503 [20] A.-G. Yin, H.-Y. Qian, J. Jia, N. Zhou, L.-Q. Tang, *Acta Cryst. Sect. E* E62 (2006) o4913.
- 504 [21] a) J.-Y. Seo, S.-H. Lee, M. Jazbinsek, H. Yun, J.-T. Kim, Y.S. Lee, I.-H. Back, F. Rotermund,  
505 O.-P. Kwon, *Cryst. Growth. Des.* 12 (2012) 313e318; b) E.I. Choi, K.J. Kim, M. Jazbinsek, J.-T.  
506 Kim, Y.S. Lee, P. Günter, S.W. Lee, O.-P. Kwon, *Cryst. Growth. Des.* 11 (2011) 3049e3055; c)  
507 R.A. Howie, T.C. Baddeley, J.L. Wardell, S.M.S.V. Wardell, *J. Mol. Struct.* 1020 (2012) 16e22;  
508 d) O.-P. Kwon, M. Jazbinsek, J.-I. Seo, P.-J. Kim, H. Yun, Y.S. Lee, P. Günter, *J. Phys. Chem.*  
509 *C* 113 (2009) 15405e15411; e) M.S. Wong, V. Gramlich, C. Boshard, P. Günter, *J. Mater.*  
510 *Chem.* 7 (1997) 2021e2026.
- 511 [22] a) R. Bosque, C. Llópez, J. Sales, X. Solans, M. Font-Bardía, *Dalton Trans.* (1994) 735e745; b)  
512 C. Llópez, R. Bosque, X. Solans, M. Font-Bardía, *New J. Chem.* 20 (1996) 1285e1292.
- 513 [24] a) A.D. Becke, *J. Chem. Phys.* 98 (1993) 5648e5652; b) C. Lee, W. Yang, R.G. Parr, *Phys. Rev.*  
514 *B* 37 (1988) 785e789.
- 515 [25] a) W.R. Wadt, P.J. Hay, *J. Chem. Phys.* 82 (1985) 284e298; b) P.J. Hay, W.R. Wadt, *J. Chem.*  
516 *Phys.* 82 (1985) 299e310.
- 517 [26] M.J. Frisch, G.W. Trucks, H.B. Schlegel, G.E. Scuseria, M.A. Robb, J.R. Cheeseman, G.  
518 Scalmani, V. Barone, B. Mennucci, G.A. Petersson, H. Nakatsuji, M. Caricato, X. Li, H.P.  
519 Hratchian, A.F. Izmaylov, J. Bloino, G. Zheng, J.L. Sonnenberg, M. Hada, M. Ehara, K. Toyota,  
520 R. Fukuda, J. Hasegawa, M. Ishida, T. Nakajima, Y. Honda, O. Kitao, H. Nakai, T. Vreven, J.A.  
521 Montgomery Jr., J.E. Peralta, F. Ogliaro, M. Bearpark, J.J. Heyd, E. Brothers, K.N. Kudin, V.N.  
522 Staroverov, T. Keith, R. Kobayashi, J. Normand, K. Raghavachari, A. Rendell, J.C. Burant, S.S.  
523 Iyengar, J. Tomasi, M. Cossi, N. Rega, J.M. Millam, M. Klene, J.E. Knox, J.B. Cross, V.  
524 Bakken, C. Adamo, J. Jaramillo, R. Gomperts, R.E. Stratmann, O. Yazyev, A.J. Austin, R.  
525 Cammi, C. Pomelli, J.W. Ochterski, R.L. Martin, K. Morokuma, V.G. Zakrzewski, G.A. Voth,  
526 P. Salvador, J.J. Dannenberg, S. Dapprich, A.D. Daniels, O. Farkas, J.B. Foresman, J.V. Ortiz, J.  
527 Cioslowski, D.J. Fox, *Gaussian 09 (Revision B.1)*, Gaussian Inc., Wallingford CT, 2010.
- 528 [27] M.E. Casida, C. Jamorski, K.C. Casida, D.R. Salahub, *J. Chem. Phys.* 108 (1998) 4439e4449.
- 529 [28] D.D. Perrin, W.L.F. Armarego, *Purification of Laboratory Chemicals*, fourth ed.  
530 Butterworth-Heinemann, Oxford, UK, 1996.
- 531 [29] G.M. Sheldrick, *SHELXS.A Program for Automatic Solution of Crystal Structure*, Univ.  
532 Goettingen, Germany, 1997.
- 533 [30] G.M. Sheldrick, *SHELX97 a Program for Crystal Structure Refinement*, Univ. Goettingen,  
534 Germany, 1997.
- 535 [31] *International Tables of X-Ray Crystallography*, vol. 4, Kynoch Press, 1974, 99e100 and 149.
- 536 [32] *APEX2*, Bruker AXS Inc., Wisconsin, USAMadison, 2007.
- 537 [33] O.V. Dolomanov, L.J. Bourhis, R.J. Gildea, J.A.K. Howard, H. Puschmann, *OLEX2: a complete*  
538 *structure solution, refinement and analysis program*, *J. Appl. Cryst.* 42 (2009) 339e341.

539 [34] a) P.C. Hariharan, J.A. Pople, Theor. Chim. Acta 28 (1973) 213e222; b) M.M. Francl, W.J.  
540 Petro, W.J. Hehre, J.S. Binkley, M.S. Gordon, D.J. DeFrees, J.A. Pople, J. Chem. Phys. 77  
541 (1982) 3654e3665.

542 [35] J.E. Rice, N.C. Handy, Int. Quantum Chem. 43 (1992) 91e118 and references therein.

543

544 .

**Legends to figures**

**Figure 1.** Representative examples of ferrocenyl and cyrhetrenyl hydrazones described previously [10,11,17].

**Scheme 1.** Synthesis of compounds  $[\text{Re}\{(\eta^5\text{-C}_5\text{H}_4)\text{eC}(\text{R}1) \frac{1}{4} \text{NeNHR}_2\}(\text{CO})_3]$  with  $\text{R}1 \frac{1}{4} \text{H}$  (4) or Me (5) and atom numbering system for NMR data.

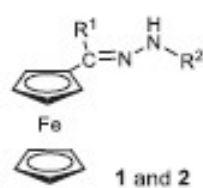
**Figure 2.** Hydrogen bonds promoted by the coordinated ethanol molecules in compound 1 (shown as light blue bonds).

**Figure 3.** ORTEP plot of the molecular structure of  $[\text{Re}\{(\eta^5\text{-C}_5\text{H}_4)\text{eC}(\text{Me}) \frac{1}{4} \text{NNH}_2\}(\text{CO})_3]$  (5c). Hydrogen atoms have been omitted for clarity.

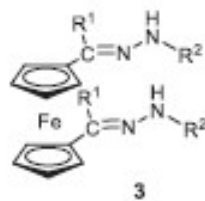
**Figure 4.** UV-visible spectra of compounds  $\text{R}_3\text{CH} \frac{1}{4} \text{NeNH}(4\text{-NO}_2\text{C}_6\text{H}_4)$  with  $\text{R}_3 \frac{1}{4}$  ferrocenyl (3a), cyrhetrenyl (4a) and phenyl (6a) in  $\text{CHCl}_3$  at 298 K.

**Figure 5.** Schematic views of the HOMO and LUMO of compounds  $\text{R}_3\text{CH} \frac{1}{4} \text{NNH}(4\text{-NO}_2\text{C}_6\text{H}_4)$  with  $\text{R}_3 \frac{1}{4}$  ferrocenyl (3a), cyrhetrenyl (4a), phenyl (6a) or cymantrenyl (7a) and the representation of the main expected transitions in their absorption spectra.

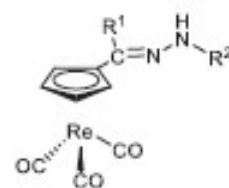
FIGURE 1



$R^1 = \text{H}(\mathbf{1}) \text{ or } \text{Me}(\mathbf{2})$   
 $R^2 = \text{substituted phenyl rings}$



$R^1 = \text{H and } R^2 = \text{CO}_2\text{Me or}$   
 $R^1 = \text{Me and } R^2 = \text{H}$



$R^1 = \text{H and}$   
 $R^2 = 2,4\text{-(NO}_2)_2\text{C}_6\text{H}_3$

# **SCHEME 1**

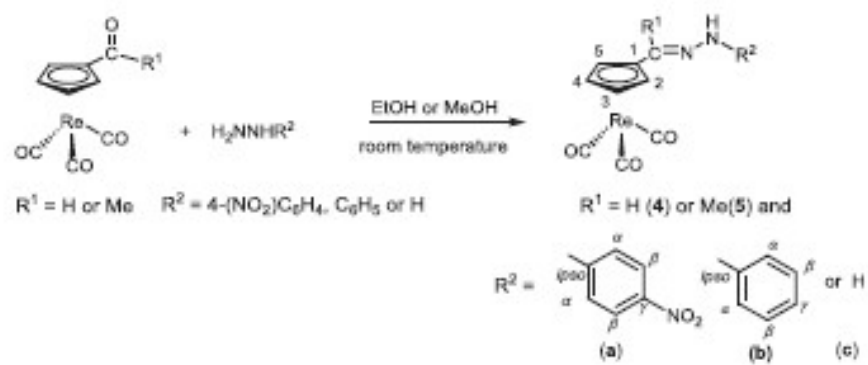
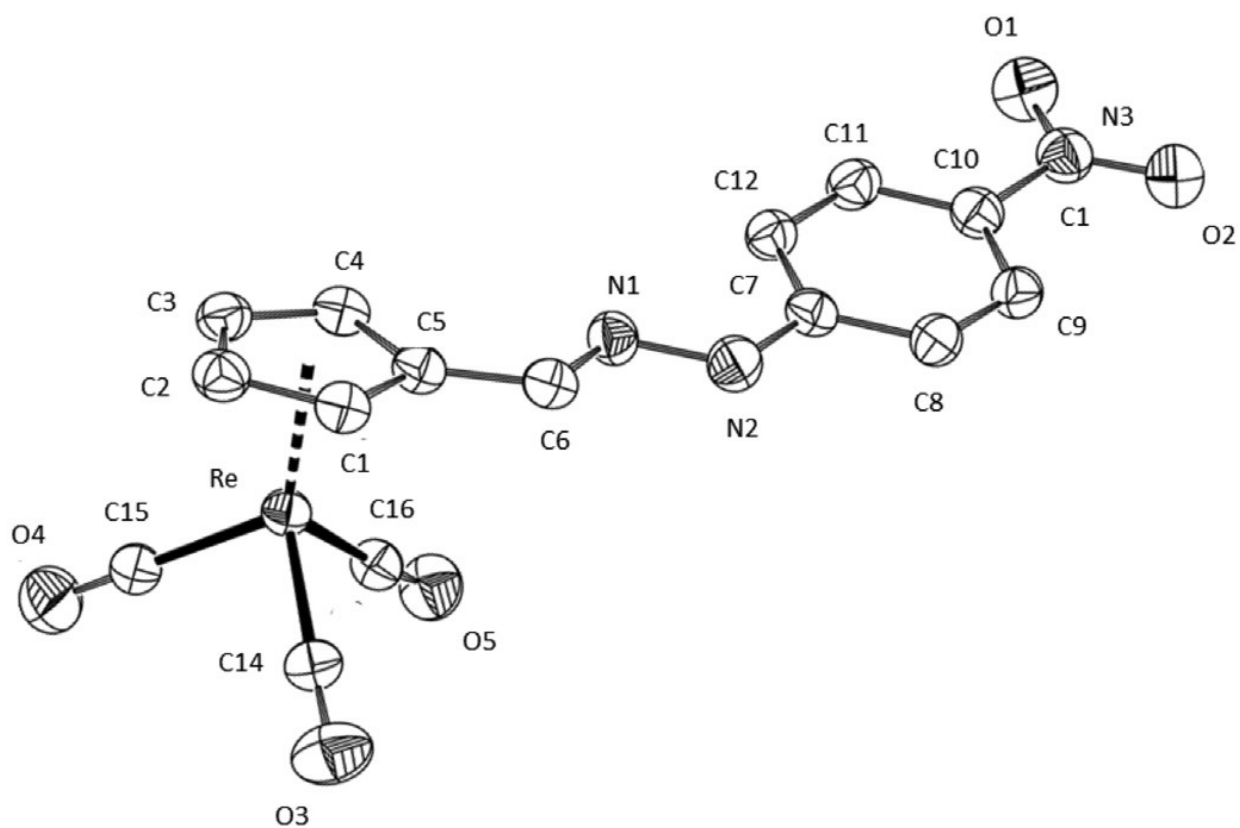
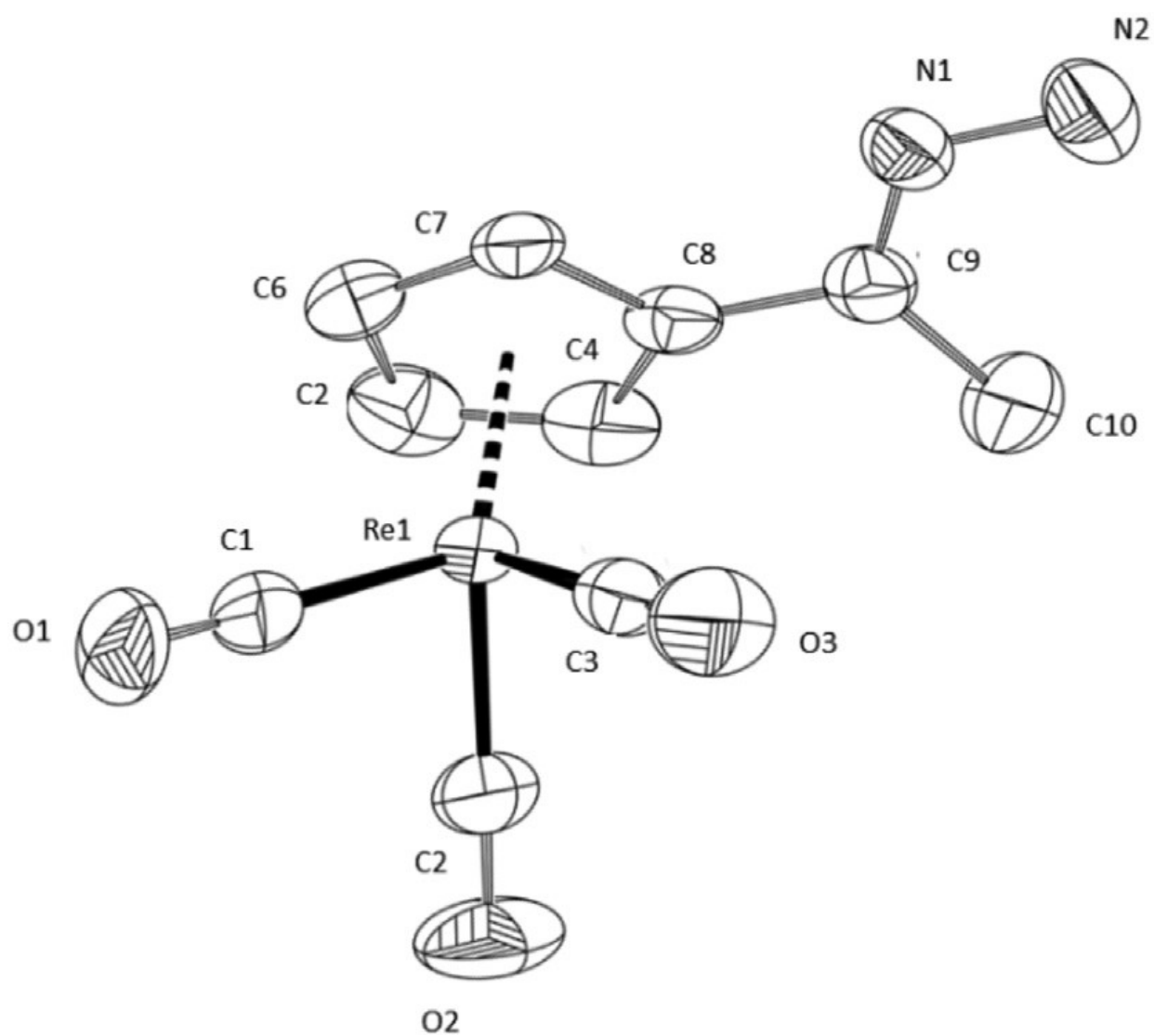


FIGURE 2



585  
586  
587

FIGURE 3.



588  
589

FIGURE 4.

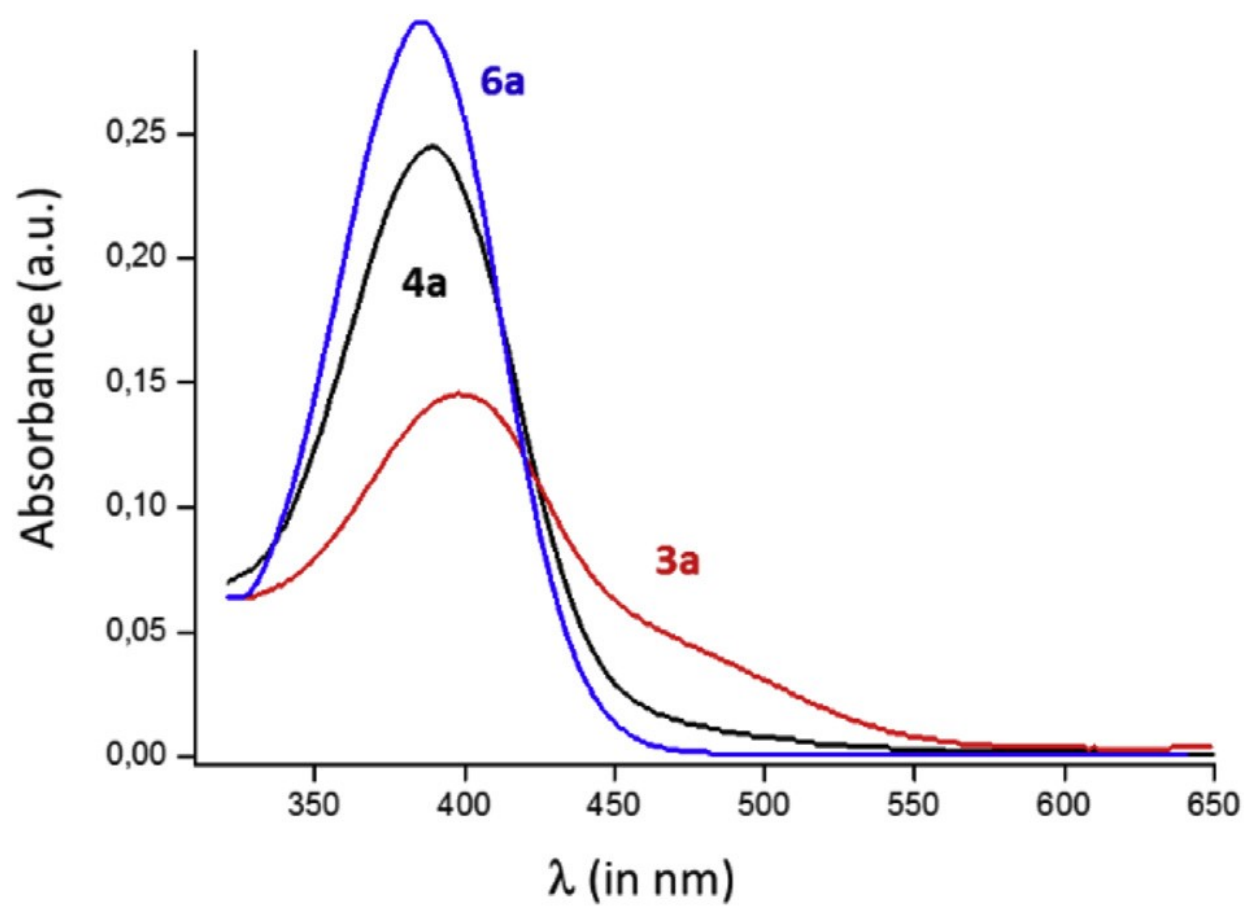
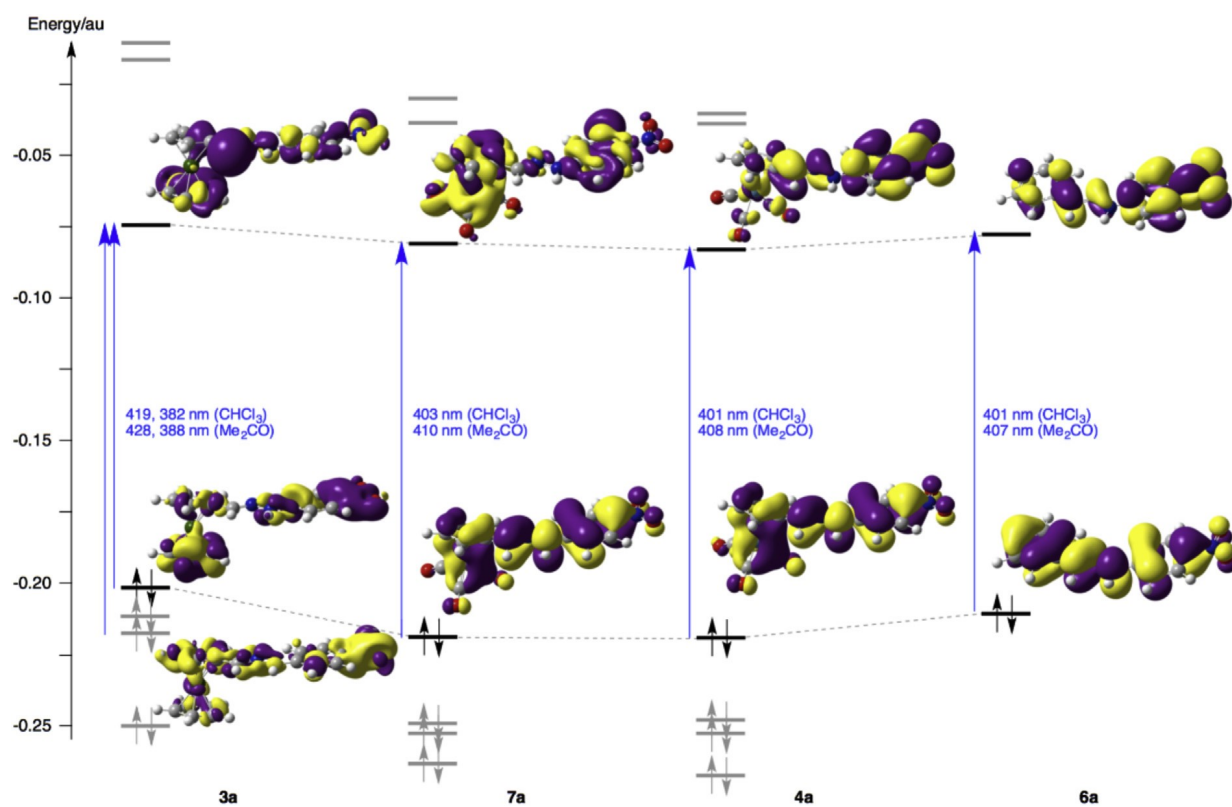




FIGURE 5.



**Table 1** Selected bond lengths (in Å) and angles (in deg.) for compounds [Re{(h5-C5H4) eC(H)  $\frac{1}{4}$  NeNH(4-NO2eC6H4)}(CO)3], (4a) and [Re{(h5-C5H4)eC(Me)  $\frac{1}{4}$  NNH2}(CO)3] (5c). [Cg(1) represents the centroid of the C5H4 ring].

4a		5c	
Re–Cg(1)	1.945(6)	Re–Cg(1)	1.9703(5)
Re–C(ring) <sup>a</sup>	2.285(14)	Re–C(ring)	2.285(14)
Re–C14	1.895(6)	Re–C1	1.907(5)
Re–C15	1.936(6)	Re–C2	1.915(5)
Re–C16	1.930(6)	Re–C3	1.910(4)
N1–N2	1.368(6)	N1–N2	1.368(6)
N1–C6	1.261(7)	N1–C9	1.275(5)
N2–C7	1.357(7)	C8–C9	1.470(6)
C5–C6	1.453(8)	C9–C10	1.500(6)
N2–C7	1.357(7)		
N3–O1	1.225(7)		
N3–O2	1.246(7)		
C14–Re–C15	91.4(3)	C1–Re–C2	88.87(9)
C14–Re–C16	90.1(3)	C1–Re–C3	89.46(9)
C15–Re–C16	91.9(3)	C2–Re–C3	89.98(9)
C9–N1–N2	118.2(4)	C9–N1–N2	118.2(4)
O1–N3–O2	124.0(6)	C8–C9–N1	116.0(4)
		C10–C9–N1	124.5(5)

<sup>a</sup> Average values.

**Table 2** Experimental Ultraviolet-visible spectroscopic data: wavelengths  $\lambda_1$  (in nm), logarithms of the molar extinction coefficients,  $\log \epsilon_1$  (in parenthesis) in chloroform, acetone and acetonitrile, for [R3 CH]NNH(4-NO<sub>2</sub>C<sub>6</sub>H<sub>4</sub>) (R3 = ¼ ferrocenyl, (3a), cyrhetrenyl (4a) or phenyl (6a).

Experimental data: $\lambda_1$ (log $\epsilon_1$ ) in				
Compound	R <sup>3</sup>	Chloroform	Acetone	Acetonitrile
3a <sup>a</sup>	Ferrocenyl	388 (4.16)	407 (4.36)	407 (4.10)
4a	Cyrhetrenyl	389 (4.39)	396 (4.43)	396 (4.27)
6a	Phenyl	385 (4.47)	389 (4.52)	389 (4.49)

<sup>a</sup> In this case, an additional shoulder at ca. 495 nm was observed in the three solvents.

**Table 3.** Summary of the results obtained from the computational studies showing. Electronic transitions with greater contributions to the absorption band detected in the UV-vis spectra of compounds, together with the position of the bands ( $\lambda$ , in nm) determined in gas phase, chloroform and acetone hydrazones 3a, 4a, 6a and 7a (the calculated oscillator strengths are given in parenthesis).

Cmpd	Assignment	Type	Gas phase	Chloroform	Acetone
3a	HOMO $\rightarrow$ LUMO [70%]	ILCT	384 (0.28)	419 (0.45)	428 (0.39)
	HOMO-2 $\rightarrow$ LUMO [70%]	MILCT	342 (0.25)	382 (0.36)	388 (0.40)
	HOMO $\rightarrow$ LUMO [22%]	ILCT	365 (0.29)	361 (0.07)	363 (0.05)
	HOMO-2 $\rightarrow$ LUMO [17%]	MILCT			
	HOMO-1 $\rightarrow$ LUMO+3 [16%]	d-d			
4a	HOMO $\rightarrow$ LUMO [98%]	ILCT	368 (0.88)	401 (0.93)	408 (0.88)
6a	HOMO $\rightarrow$ LUMO [100%]	ILCT	366 (0.90)	401 (0.95)	407 (0.91)
7a	HOMO $\rightarrow$ LUMO [47%]	ILCT	376 (0.42)	403 (0.87)	410 (0.84)
	HOMO $\rightarrow$ LUMO [21%]	ILCT	371 (0.19)		
	HOMO-1 $\rightarrow$ LUMO+1 [19%]	MILCT			
	HOMO-2 $\rightarrow$ LUMO+2 [14%]	d-d			
	HOMO $\rightarrow$ LUMO [16%]	ILCT	347 (0.16)	—	—
	HOMO-3 $\rightarrow$ LUMO+1 [15%]	MILCT			
	HOMO-3 $\rightarrow$ LUMO+3 [12%]	d-d			
	HOMO $\rightarrow$ LUMO [15%]	ILCT	343 (0.11)		
	HOMO-1 $\rightarrow$ LUMO+2 [12%]	d-d			
	HOMO-2 $\rightarrow$ LUMO+3 [12%]	d-d			

**Table 4.** Summary of crystallographic data and details of the refinement of the crystal structures of compounds  $[\text{Re}\{(\text{h}5\text{-C}_5\text{H}_4)\text{eC}(\text{H})\frac{1}{4}\text{NeNH}(4\text{-NO}_2\text{eC}_6\text{H}_4)\}(\text{CO})_3]$  (4a) and  $[\text{Re}\{(\text{h}5\text{-C}_5\text{H}_4)\text{eC}(\text{Me})\frac{1}{4}\text{NeNH}_2\}(\text{CO})_3]$  (5c).

	4a	5c
Crystal size/mm × mm × mm	0.2 × 0.1 × 0.1	0.312 × 0.152 × 0.068
Empirical formula	$\text{C}_{15}\text{H}_{10}\text{N}_2\text{O}_5\text{Re}$	$\text{C}_{10}\text{H}_6\text{N}_2\text{O}_3\text{Re}$
Formula weight	498.46	391.39
Crystal system	Monoclinic	Monoclinic
Space group	$P2_1/c$	$P2_1/c$
<i>a</i> /Å	11.592(5)	10.911(4)
<i>b</i> /Å	10.920(3)	8.293(3)
<i>c</i> /Å	12.448(4)	13.520(2)
$\alpha$ /deg	90.0	90.0
$\beta$ /deg	99.15	220.201
$V/\text{\AA}^3$	1555.7(9)	1148(79)
<i>Z</i>	4	4
<i>T</i>	293(1)	296.15
$D_{\text{calc}}/\text{mg} \times \text{mm}^{-3}$	2.128	2.264
$\mu/\text{mm}^{-1}$	7.842	10.576
<i>R</i> (000)	944	728.0
$\theta$ range for data collection/deg.	From 1.78 to 30.30	From 2.93 to 26.4
N. of collected reflections	11,801	24,902
N. of unique reflect. [ <i>R</i> (int.)]	3765 [0.0488]	2336 [0.0210]
N. of data	3765	2363
N. of parameters	218	147
Goodness of fit on $F^2$	1.141	1.396
Final <i>R</i> indexes [ <i>I</i> > 2 $\sigma$ ( <i>I</i> )]	$R_1 = 0.0362$ , $wR_2 = 0.0981$	$R_1 = 0.0152$ , $wR_2 = 0.0445$
Final <i>R</i> indexes (all data)	$R_1 = 0.0432$ , $wR_2 = 0.1022$	$R_1 = 0.0193$ , $wR_2 = 0.0619$